Blue Fluorescent Polyamides Containing Naphthalene and Oxadiazole Rings

MARIANA-DANA DAMACEANU, RADU-DAN RUSU, ALINA NICOLESCU, MARIA BRUMA

"Petru Poni" Institute of Macromolecular Chemistry, Polycondensation and Physical Characterization of Polymers Departments, Aleea Grigore Ghica Voda 41A, Iasi-700487, Romania

Received 10 November 2010; accepted 15 November 2010
DOI: 10.1002/pola.24500
Published online 14 December 2010 in Wiley Online Library (wileyonlinelibrary.com).

ABSTRACT: New polyamides containing 1,3,4-oxadiazole and naphthalene rings were prepared by low-temperature solution polycondensation reaction of a new diamine containing preformed oxadiazole ring with various aromatic diacid chlorides. Elemental analysis, mass, infrared, and nuclear magnetic resonance spectroscopy were used to confirm the structure of the monomers and corresponding polymers. The thermal stability and glass transition temperatures of these poly(oxadiazole-amide)s were measured and compared with those of related polymers. Their good solubility allows them to be processed in very thin films with smooth surfaces, without pinholes or cracks, when studied by atomic force microscopy. Upon irradiation with UV light the polymers showed photoluminescence maxima in the blue spectral range, both in solution and in solid state. Cyclic voltammetry (CV) was performed in order to obtain information about the electrochemical stability and reversibility of the redox processes of these polyamides. The highest occupied molecular orbital and the lowest unoccupied molecular orbital energy levels, and electrochemical and optical band gap values were calculated by using the results of CV and UV/vis, respectively, showing very good electron and hole injection and transport characteristics. These properties make the present polymers suitable for application in electroluminescent devices. © 2010 Wiley Periodicals, Inc. J Polym Sci Part A: Polym Chem 49: 893–906, 2011

KEYWORDS: electrochemistry; fluorescence; new oxadiazole monomer; polyamides; smooth thin films

INTRODUCTION Aromatic polyamides are considered to be high-performance materials due to their superior thermal and mechanical properties, which make them useful for advanced technologies.[1] There is an increasing demand for use as advantageous replacements for metals or ceramics in currently used goods, or even as new materials in novel technological applications: advanced fabrics, coatings, and fillers, advanced composites in the aerospace and armament industry, asbestos substitutes, electrical insulation, bullet-proof body armor, industrial filters, and protective and sport clothing, among others.[2–4] However, the extremely high transition temperatures of the commercial aramids, which lie above their decomposition temperatures, and their poor solubility in common organic solvents give rise to processing difficulties and limit their applications.[5,6] As a consequence, recent basic and applied research has focused on enhancing their processability and solubility to broaden the scope of the technological applications of these materials. Attempts to increase the solubility of aromatic polyamides employed a variety of methods to chemically modify their structure, such as through the introduction of bulky, packing-disruptive groups in the polymer chain or as side groups,[7–10] the incorporation of flexible chains into the polyamide backbone,[11–13] or the use of meta-oriented or asymmetrically substituted monomers.[14–17] Conventionally, the modified polyamides and polyimides have been prepared by using diamine monomers containing flexible groups.[18–21] Also, it has been demonstrated that incorporation of both ether and naphthyl units into the polymer backbones may enhance the solubility and processability of thermally stable polymers including aromatic polyamides and polyimides without any significant reduction in thermal stability. In continuing the preparation of new high-performance, processable polyamides, it is of interest to synthesize processable polyamides with high temperature resistance.

Fully aromatic poly(1,3,4-oxadiazole)s form another class of high performance polymers that are designated for use in small quantities, but with very high end-value.[22] High performances include high thermal resistance in oxidative atmosphere, good hydrolytic stability, tough mechanical properties, optical properties, highly ordered systems, and other special properties determined by the electronic structure of this particular heterocycle.[23–26] There is currently much interest in high-brightness blue light-emitting diodes to be used in full colour displays, full colour indicators, and light sources for lamps, which have high efficiency and high reliability as characteristics. For such a purpose polyoxadiazoles are very attractive because, due to the electron-withdrawing character of the 1,3,4-oxadiazole rings, they can

Correspondence to: M.-D. Damaceanu (E-mail: damaceanu@icmpp.ro)
Journal of Polymer Science: Part A: Polymer Chemistry, Vol. 49, 893–906 (2011) © 2010 Wiley Periodicals, Inc.

facilitate electron injection and transport. But the applicability of these polymers is limited because they have rigid molecules due to the delocalization of π-electrons along the polymer chain, which makes them insoluble in organic solvents and free of or with too high glass transition temperature, and therefore their processing is very difficult.[27] Research of poly(1,3,4-oxadiazole)s has considerably extended in the last years as can be seen from the large number of publications and patents in this field. Most of this research aims to improve solubility and processability of aromatic polyoxadiazoles by introduction of certain substituents on aromatic rings, flexible bridges in the polymer chain or voluminous units pendant to the chain, provided that the conjugation is not disturbed and the high-performance properties are not affected.[28,29]

The combination of these structural modifications, that is, the incorporation of 1,3,4-oxadiazole rings, naphthalene units and flexible groups in the polymer backbones, minimizes the trade-off between the processability and properties of wholly aromatic polyamides. In our continuing efforts to develop processable high-performance polymers with potential applications in electroluminescent devices, this work describes the successful synthesis of a series of poly(oxadiazole-amide)s based on a new monomer containing 1,3,4-oxadiazole ring and both ether and naphthalene moieties and three different diacid chlorides containing solubility improving flexible groups. The properties of these poly(oxadiazole-amide)s such as solubility, molecular weights, thermal stability, glass transition temperature, photo-optical, and electrochemical properties, as well as the quality of the thin films obtained from these polymers were investigated.

EXPERIMENTAL

Starting Materials

5-Amino-naphthol (97%), 4-fluorobenzoic acid (98%), diphenyl-dichlorosilane (≥98%; GC), 4,4′-(hexafluoroisopropylidene)bis(benzoic acid) (98%), *p*-bromotoluene (98%), 4,4′-oxybis(benzoic acid) (99%), chromium oxide (98%), hydrazine hydrate (reagent grade), 1-methyl-2-pyrrolidinone (HPLC grade; NMP), *N*,*N*-dimethylacetamide (HPLC grade; DMAc), dimethylsulfoxide (99.7%; DMSO), anhydrous *N*,*N*-dimethylformamide (99.8%; DMF), anhydrous tetrahydrofuran (99%), *n*-hexane (99.5%), lithium (dispersion in mineral oil, 99.95%) and thionyl chloride (99%) were purchased from Sigma-Aldrich (Taufkirchen, Germany). Acetic anhydride (98%; GC) and pyridine (99.5%; GC) were purchased from Merck (Darmstadt, Germany). Chloroform (95%) and potassium carbonate (reagent grade) were purchased from Chimopar (Bucharest, Romania). Sulfuric acid (98%) and ethanol (96%) were purchased from Chemical Company (Iasi, Romania). All reagents were used without further purification. Solvents were purified by standard procedures and handled in a moisture-free atmosphere.

Synthesis of Monomers

The new oxadiazole-containing monomer and polymers were synthesized as shown in Schemes 1 and 2, respectively. The detailed synthetic procedures are as follows.

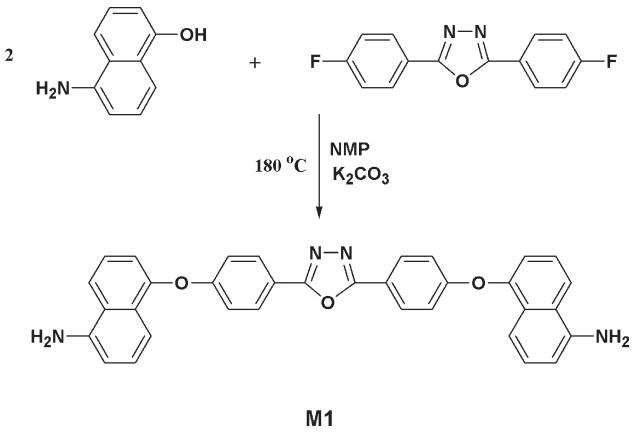

M1

SCHEME 1 Synthesis of the diamino-oxadiazole **M1**.

2,5-Bis-[4-(5-amino-naphthalene-1-yloxy)-phenyl]-1,3,4-oxadiazole (M1)

2,5-Bis(*p*-fluorophenyl)-1,3,4-oxadiazole (7.74 g, 30 mmol), which was prepared from 4-fluorobenzoic acid and hydrazine hydrate by a previously reported procedure,[30] 5-amino-naphthol (10.1 g, 63 mmol) and potassium carbonate (13.8 g, 100 mmol) were added, sequentially, while maintaining good stirring, to a 250 mL three-necked round-bottomed flask, containing 80 mL of 1-methyl-2-pyrrolidinone (NMP), equipped with a mechanical stirrer, nitrogen inlet and outlet and a Dean-Stark trap under a reflux condenser. The reaction mixture was stirred and heated to 180 °C, and maintained at this temperature, under a gentle nitrogen flow, for 40 h for complete conversion. During this time, progress of the reaction was monitored by thin-layer chromatography (TLC). The reaction mixture was gradually cooled to room temperature and poured into water in order to precipitate the solid compound. The dark violet monomer was washed with plenty of water and then purified by recrystallization using coprecipitation in *N*,*N*-dimethylformamide and water in order to remove the unreacted starting compounds and the high boiling solvent. Finally, 2,5-bis-[4-(5-amino-naphthalene-1-yloxy)-phenyl]-1,3,4-oxadiazole (**M1**) was obtained as dark violet crystals after drying in an oven, under vacuum, at 100 °C for 6 h. Yield: 10.13 g (63%). mp: 183–185 °C. ^{1}H NMR (DMSO, 25 °C), δ (ppm): 5.89 (4H, s,NH_2), 6.73 (2H, d, 7.6 Hz, H-8,), 7.08 (2H, d, 8.4 Hz, H-10), 7.12 (4H, d, 8.8 Hz, H-12), 7.18 (2H, d, 6.8 Hz, H-3), 7.21 (2H, t, 8 Hz, H-9), 7.40 (2H, t, 7.6 Hz, H-2), 8.01 (2H, d, 8.4 Hz, H-1), 8.07 (4H, d, 8.8 Hz, H-13). ^{13}C NMR (DMSO, 25 °C), δ (ppm): 108.17 (C-8), 108.34 (C-10), 116.18 (C-3), 117.27 (C-12), 117.47 (C-14), 119.84 (C-1), 123.44 (C-2), 124.27 (C-6), 127.49 (C-9), 129.59 (C-5), 128.79 (C-13), 145.31 (C-7), 150.21 (C-4), 161.24 (C-11), 163.41 (C-15). ^{15}N NMR (DMSO, 25 °C), δ (ppm): 60.2 (NH_2). FTIR (KBr, powder, cm^{-1}): 3443, 3381, (NH stretch), 3063 (Ar—H stretch), 1612 (NH stretch), 1488 (aromatic C=C stretch), 1275 (C—N stretch), 1246, 1165 (—C—O—C— stretch), 1009, 960 (oxadiazole stretch), 780 (NH_2 wag). MS (ESI, m/z): calcd for $C_{34}H_{24}N_4O_3$, 536.5794; found, 537.4023 [M + H]. Anal calcd for $C_{34}H_{24}N_4O_3$: C,

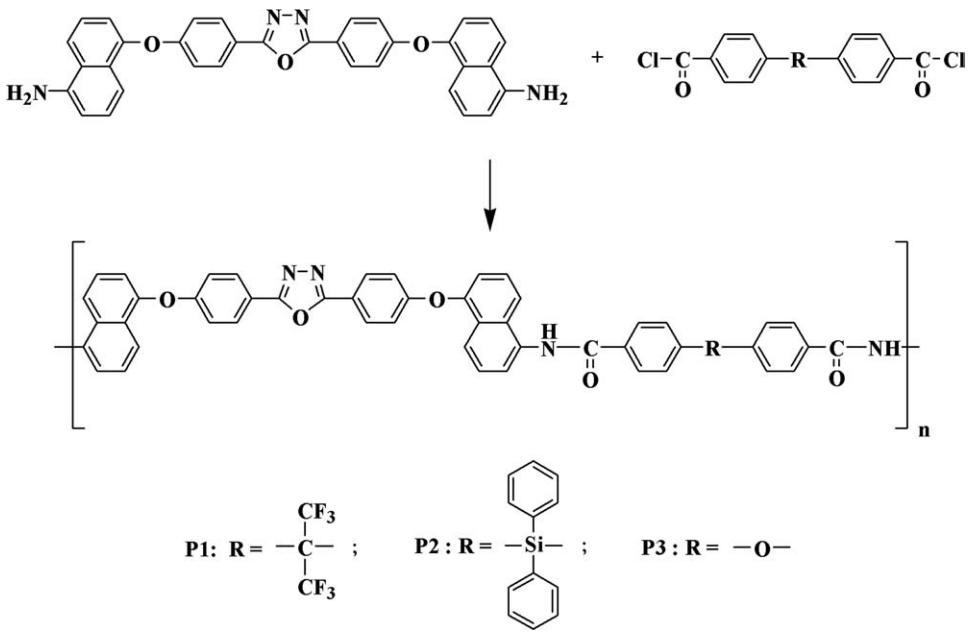

SCHEME 2 Synthesis of poly(oxadiazole-amide)s.

76.09; H, 4.52; N, 10.44; O, 8.95. Found: C, 76.31; H, 4.35; N, 10.58; O, 8.76.

4,4′-(Hexafluoroisopropylidene)bis(benzoyl chloride) (M2)

The fluorine-containing diacid chloride **M2** was prepared by treating the corresponding 4,4′-(hexafluoroisopropylidene)-bis(benzoic acid) with excess thionyl chloride at reflux.[31] It was purified by recrystallization from *n*-hexane. Yield: 74%. mp: 93–94 °C (lit. mp: 93-94 °C). ^{1}H NMR (DMSO, 25 °C), δ (ppm): 7.46 (4H, d, 8.4 Hz), 8.04 (4 H, d, 8.4 Hz). ^{13}C NMR (DMSO, 25 °C), δ (ppm): 64.21 (septet, 25 Hz), 123.73 (quartet, 285 Hz), 129.72, 130.05, 132.05, 136.23, 166.46.

Bis(p-chlorocarbonyl-phenylene)-diphenylsilane (M3)

The silicon-containing diacid chloride **M3** was prepared by a multi-step reaction.[32] First, *p*-bromotoluene reacted with lithium to give *p*-tolyl-lithium which further reacted with diphenyl-dichlorosilane to produce bis(*p*-tolyl)-diphenylsilane. The later was oxidized with chromium oxide in a mixture of sulfuric acid and acetic anhydride and gave the corresponding bis(*p*-carboxyphenylene)-diphenysilane which was further treated with excess thionyl chloride at reflux to result in bis(*p*-chlorocarbonyl-phenylene)-diphenylsilane. The final product was purified by recrystallization from ligroin. Yield: 71%. mp: 181–183 °C (lit. mp: 184–185 °C). ^{1}H NMR (DMSO, 25 °C), δ (ppm): 7.43 (4H, t, 7.9 Hz), 7.47 (4H, d, 7.6 Hz), 7.49 (2H, t, 7.6 Hz), 7.61 (4H, d, 8.4 Hz), 7.99 (4H, d, 8.0 Hz). ^{13}C NMR (DMSO, 25 °C), δ (ppm): 128.44, 128.78, 130.30, 132.23, 132.34, 135.89, 136.07, 138.89, 167.24.

4,4′-Oxybis(benzoyl chloride) (M4)

The ether bridge-containing diacid chloride **M4** was prepared by treating the corresponding 4,4′-oxybis(benzoic acid) with excess thionyl chloride at reflux, in the presence of *N*,*N*-dimethylformamide as reaction catalyst.[33] It was purified by recrystallization from *n*-hexane. Yield: 80%. mp: 93 °C (lit. mp: 94 °C). ^{1}H NMR (DMSO, 25 °C), δ (ppm): 7.17 (4H, d, 8.8 Hz), 8.00 (4H, d, 8.8 Hz). ^{13}C NMR (DMSO, 25 °C), δ (ppm): 118.71, 126.43, 131.81, 159.49, 166.63.

Synthesis of Polymers

Poly(1,3,4-oxadiazole-amide)s **P1–P3** have been synthesized by low-temperature solution polycondensation reaction of equimolar amounts of the aromatic diamine containing oxadiazole and naphthalene rings, **M1**, with diacid chlorides **M2–M4** having hexafluoroisopropylidene, silicon, or ether groups, respectively, using NMP as a solvent and with pyridine as an acid acceptor. The relative amounts of monomers and NMP were adjusted so as to have a solid content of 10–15%.

A typical reaction was carried out as follows. Diamine **M1** (2.68 g, 5 mmol), 28 mL NMP and 0.5 mL of pyridine, were placed in a 100 mL three-necked flask equipped with a mechanical stirrer and a nitrogen inlet and outlet and the mixture was stirred under nitrogen until complete dissolution. The solution was cooled to −10 °C and hexafluoroisopropylidene-containing diacid chloride **M2** (2.145 g, 5 mmol) was added with rapid stirring. The content of the flask was kept below 0 °C for 15 min. The cooling bath was then removed and the reaction mixture was allowed to reach room temperature after which it was stirred for additional 6 h at this temperature. The resulting dark violet solution of poly(1,3,4-oxadiazole-amide), **P1**, was poured into water to precipitate the solid polymer. The dark violet polymer was washed with plenty of water and finally treated with ethanol in a Soxhlet apparatus for 1 day to remove the unreacted monomers and oligomers and the high boiling solvent. Finally, poly(1,3,4-oxadiazole-amide) **P1** was obtained as a light violet powder after drying in an oven under vacuum, at 100 °C for 6 h.

Polymer P1

Yield: 3.05 g (68%). ^{1}H NMR (DMSO, 25 °C), δ (ppm): 7.23 (4H, d, 8.0 Hz, H-12), 7.30 (2H, d, 6.8 Hz, H-3), 7.53–7.64 (8H, m, H-2 + H-9 + H19), 7.73 (2H, d, 6.4 Hz, H-8), 7.90–8.00 (4H, m, H-1 + H-10), 8.13 (4H, d, 7.6 Hz, H-13), 8.26 (4H, d, 8.0 Hz, H-18), 10.69 (2H, s, amide—NH). ^{13}C NMR (DMSO, 25 °C), δ (ppm): 64.11 (septet, 25 Hz, C-21), 116.04 (C-3), 117.82 (C-12), 118.02 (C-14), 119.71 (C-10), 120.43 (C-1), 123.78 (quartet, 285 Hz, C-22), 124.78 (C-8), 126.18, 126.26 (C-2 + C-9), 127.09 (C-5), 128.28 (C-18), 128.90 (C-13), 129.83 (C-19), 130.83 (C-6), 134.07 (C-7), 135.12 (C-20), 135.54 (C-17), 150.74 (C-4), 160.72 (C-11), 163.40 (C-15), 165.37 (C-16). ^{15}N NMR (DMSO, 25 °C), δ (ppm): 121.4 (amide NH). Anal calcd for $C_{51}H_{30}F_6N_4O_5$: C, 68.60; H, 3.39; F, 12.77; N, 6.28; O, 8.96. Found: C, 68.73; H, 3.45; F, 12.63; N, 6.39; O, 8.80.

Polymer P2

Yield: 2.66 g (72%). ^{1}H NMR (DMSO, 25 °C), δ (ppm): 7.05–7.26 (4H, bs), 7.26–7.35 (2H, bs), 7.40–7.57 (10H, m), 7.57–7.65 (4H, bs), 7.65–7.80 (6H, bs), 7.85–8.00 (4H, m), 8.13 (4H, d, 8.4Hz), 8.19 (4H, d, 7.2 Hz), 10.6 (2H, bs, amide-NH). ^{13}C NMR (DMSO, 25 °C), δ (ppm): 116.02, 117.78, 117.99, 119.57, 120.42, 124.70, 126.12, 126.24, 127.08, 127.36, 128.32, 128.87, 130.17, 130.84, 132.54, 134.21, 135.82, 135.92, 137.50, 150.71, 160.72, 163.38, 166.15. ^{15}N NMR (DMSO, 25 °C), δ (ppm): 121.3 (amide NH). Anal calcd for $C_{60}H_{40}N_4O_5Si$: C, 77.89; H, 4.37; N, 6.06; O, 8.64; Si, 3.04. Found: C, 78.06; H, 4.48; N, 6.13; O, 8.48; Si, 2.85.

Polymer P3

Yield: 2.43 g (80%). ^{1}H NMR (DMSO, 25 °C), δ (ppm): 7.24 (4H, d, 8.8 Hz), 7.28–7. 33 (6H, m), 7.62 (4H, t, 7.6 Hz), 7.72 (2H, d, 7.2 Hz), 7.96 (4H, d, 8 Hz), 8.15 (4H, d, 8.4 Hz), 8.23 (4H, d, 8.4 Hz), 10.54 (2H, bs, amide-NH). ^{13}C NMR (DMSO, 25 °C), δ (ppm): 116.12, 117.81, 118.01, 118.57, 119.58, 120.57, 124.93, 126.17, 126.33, 127.11, 128.95, 129.80, 130.28, 131.02, 134.40, 150.70, 158.85, 160.80, 163.43, 165.38. ^{15}N NMR (DMSO, 25 °C), δ (ppm): 120.1 (amide NH). Anal calcd for $C_{48}H_{30}N_4O_6$: C, 75.97; H, 3.99; N, 7.39; O, 12.65. Found: C, 76.12; H, 3.95; N, 7.50; O, 12.43.

Preparation of Polymer Films

Very diluted polymer solutions in NMP with concentration of 1% were used to obtain very thin films having the thickness in the range of nanometers onto silicon wafers, by spin-coating technique, at a speed of 5000 rpm. These films, as deposited, were gradually heated from room temperature up to 180 °C, and kept at 180 °C for 1 h to remove the residual solvent and were used for atomic force microscopy (AFM) investigations.

Measurements

The NMR spectra have been recorded on a Bruker Advance III 400 spectrometer, equipped with a 5 mm multinuclear inverse detection probe, operating at 400.1, 100.6, and 40.6 MHz for ^{1}H, ^{13}C, and ^{15}N nuclei, respectively. ^{1}H and ^{13}C chemical shifts are reported in δ units (ppm) relative to the residual peak of solvent (ref: DMSO, ^{1}H, 2.51 ppm; ^{13}C, 39.47 ppm). H,H-COSY, H,C-HSQC, and H,C-HMBC experiments were recorded using standard pulse sequences in the version with *z*-gradients, as delivered by Bruker with TopSpin 2.1 PL6 operating software. The ^{15}N chemical shifts were obtained as projections from the 2D indirectly detected H,N-HMQC spectra, using standard pulse sequences in the version with *z*-gradients as delivered by Bruker and are referred to external liquid ammonia (0.0 ppm) using as external standard nitromethane (380.2 ppm).

Mass spectral (MS) data were collected on an Agilent 6520 Accurate Mass ESI Q-ToF Liquid Chromatography/Mass Spectrometer. Elemental analysis was performed on an Elemental Analyzer CHNS 2400 II Perkin Elmer.

The inherent viscosities of the polymers were determined at 20 °C, by using NMP-polymer solutions of 0.5 g/dL concentration, with an Ubbelohde viscometer. The infrared (FTIR) spectra were recorded on FT-IR Bruker Vertex 70 Spectrophotometer in transmission mode, by using KBr pellets.

Average-molecular weights were measured by means of gel permeation chromatography (GPC) using a PL-EMD 950 evaporative mass detector instrument. Polystyrene standards of known molecular weight were used for calibration and dimethylformamide as the mobile phase.

The thermal stability of the polymers was investigated by thermogravimetric analysis (TGA) using a STA 449F1 Jupiter derivatograph (Netzsch), operating at a heating rate of 10 °C/min, in nitrogen atmosphere, from room temperature to 700 °C. The onset on the TG curve was considered to be the beginning of decomposition or the initial decomposition temperature (IDT). The temperature of maximum rate of decomposition which is the maximum signal in differential thermogravimetry (DTG) curves was also recorded.

The glass transition temperature (T_g) of the precipitated polymers was determined by using a Pyris Diamond DSC Perkin Elmer calorimeter. Approximately 3 to 8 mg of each polymer were crimped in aluminum pans and run in nitrogen with a heat-cool-heat profile from room temperature to 380 °C at 10 °C/min. The midpoint temperature of the change in slope of the DSC signal of the second heating cycle was used to determine the glass transition temperature values of the polymers.

The quality of very thin films as-deposited on silicon plates was investigated by atomic force microscopy (AFM) using a Scanning Probe Microscopy Solver PRO-M, NT-MDT equipment made in Russia, in semi-contact mode, semi-contact topography technique.

The UV–vis absorption and photoluminescence spectra of polyamides were registered with Specord M42 apparatus and Perkin Elmer LS 55 apparatus, respectively, by using very diluted polymer solutions ($\sim 10^{-5}$ M) or very thin films cast from NMP solutions.

Cyclic voltammetry (CV) was performed on a Bioanalytical System, Potentiostat-Galvanostat (BAS 100B/W). The electrochemical cell was equipped with three-electrodes: a working electrode (ITO-coated glass with 2.5 × 2.5 cm^2 area covered

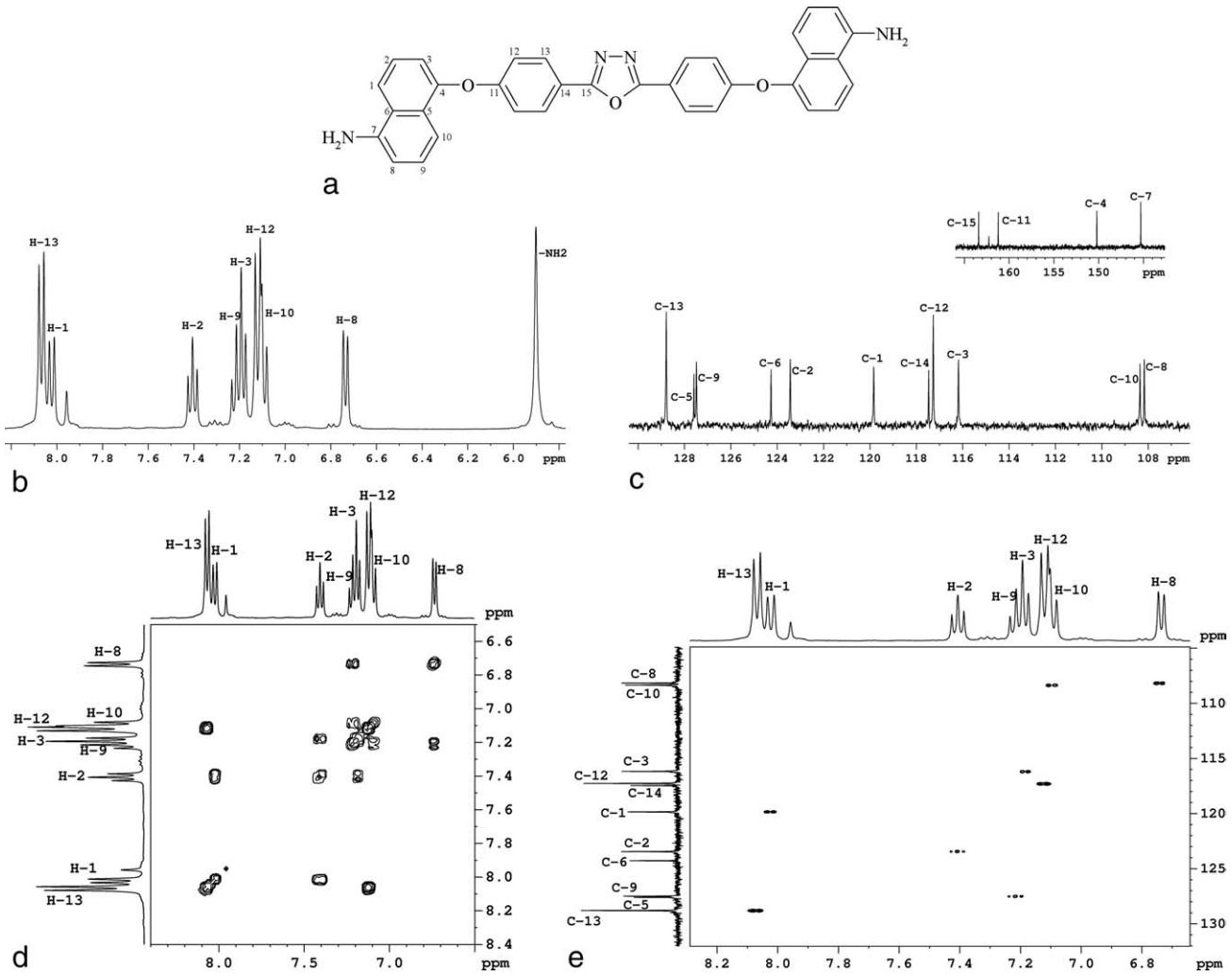

FIGURE 1 NMR spectra of monomer **M1** in DMSO-d_6: (a) numbering scheme; (b) ^{1}H NMR spectrum; (c) ^{13}C NMR spectrum; (d) H,H-COSY spectrum; (e) H,C-HSQC spectrum.

with the polymer films), an auxiliary electrode (platinum wire) and a reference electrode (silver wire coated with AgCl). All potentials were reported with respect to Ag/AgCl electrode at room temperature under a nitrogen atmosphere. Ferrocene was used as an external reference for calibration (+0.425 vs. Ag/AgCl). Tetrabutylammonium perchlorate (TBAP)/acetonitrile (CH_3CN) was used as supporting electrolyte.

RESULTS AND DISCUSSION

A new oxadiazole-containing aromatic diamine, namely 2,5-bis-[4-(5-amino-naphthalene-1-yloxy)-phenyl]-1,3,4-oxadiazole (**M1**), was successfully prepared in one step by aromatic nucleophilic substitution reaction of 2,5-bis(*p*-fluorophenyl)-1,3,4-oxadiazole, which was synthesized by a previously reported procedure,[30] with two-fold molar amounts of 5-amino-1-naphthol, in the presence of K_2CO_3 (Scheme 1).

This method is based on the nucleophilic displacement of the activated fluoro-substituents by potassium phenoxide, in polar aprotic solvents such as DMAc or NMP. The oxadiazole moiety can accept a negative charge and lower the activation energy for the displacement of the *p*-substituted fluoro group through a Meisenheimer complex, analogous to conventional activating groups such as ketone or sulfone.

Basic Characterization

This new compound was characterized by elemental analysis, MS, IR, ^{1}H and ^{13}C NMR spectroscopy, thereby fully proving the chemical structure of this monomer. In IR spectra **M1** revealed characteristic absorption bands of the functional groups at 3443 and 3381 (NH stretching), 3063 (aromatic C—H stretching), 1612 (NH stretching), 1488 (aromatic C=C stretching), 1275 (C—N stretching), 1246 and 1165 (—C—O—C— stretching), 1009 and 960 (=C—O—C= stretching in oxadiazole rings), 780 cm^{-1} (NH_2 wagging), confirming the presence of 1,3,4-oxadiazole ring, ether linkage and primary amine groups in the product. Figure 1(b,c) illustrates the ^{1}H NMR and ^{13}C NMR spectra corresponding to the new oxadiazole compound (**M1**). The assignments for

TABLE 1 FTIR (KBr Pellets, cm^{-1}) Data of the Synthesized Polyamides

Band Assign	P1	P2	P3
N—H[a]str	3434	3424	3424
Amide I, C=O[a]str.	1668	1667	1664
Amide II, N—H[a]str.	1529	1524	1528
Oxadiazole, C—O—C[a]str.	969	959	947
Oxadiazole, C—O—C[a]str.	1015	1014	1011
[b]Ar. C—H[a]str.	3070	3067	3066
[b]Ar. C=C[a]str.	1489	1488	1489
[b]Ar. C—O—C[c]asym.	1240	1239	1240
[b]Ar. C—O—C[d]sym.	1167	1165	1166

[a] str: Stretching.
[b] Ar: Aromatic.
[c] asym: Asymmetric stretching.
[d] sym: Symmetric stretching.

the ^{1}H and ^{13}C chemical shifts were made according to the numbering scheme presented in Figure 1(a). These assignments are based on 2D NMR homo- and heteronuclear correlations. Thus, the *J*-coupled protons were assigned from H,H-COSY (Correlation Spectroscopy) spectrum presented in Figure 1(d). The assignments of the carbons from CH groups were based on H,C-HSQC (Heteronuclear Single Quantum Coherence) spectrum presented in Figure 1(e). The quaternary carbons were identified from H,C-HMBC (Heteronuclear Multiple Bond Coherence) spectrum.

Low-temperature solution polycondensation reaction of aromatic diamine, 2,5-bis-[4-(5-amino-naphthalene-1-yloxy)-phenyl)-1,3,4-oxadiazole, **M1**, with 4,4′-(hexafluoroisopropylidene)bis(benzoyl chloride), **M2**, bis(*p*-chlorocarbonyl-phenylene)-diphenylsilane, **M3**, or 4,4′-oxybis(benzoyl chloride), **M4**, gave aromatic poly(oxadiazole-amide)s containing hexafluoroisopropylidene groups, **P1**, diphenylsilane units, **P2**, or ether bridges, **P3**, respectively, as seen in Scheme 2. This simple, well-known method allows obtaining highly pure materials required in optoelectronic applications without the use of any difficult to remove catalyst. The polymerization proceeded homogeneously throughout the reaction and afforded clear, highly viscous polymer solutions. The poly(oxadiazole-amide)s precipitated in a tough, fiber-like form when the resulting polymer solutions were slowly poured into water.

The structures of the polymers were identified by means of elemental analysis, IR, ^{1}H NMR, and ^{13}C NMR spectroscopy. The FTIR spectra of the synthesized poly(oxadiazole-amide)s provided evidence that all of the naphthalene units, oxadiazole rings and amide groups were successfully incorporated into the polymer chain, as listed in Table 1. All the polymers showed characteristic amide group absorptions in the range of 3450–3200 cm^{-1} (NH stretching, wide bands), 1670–1660 cm^{-1} (carbonyl stretching, amide I), and 1530–1520 cm^{-1} (NH deformation, amide II). Characteristic absorption peaks of 1,3,4-oxadiazole ring were also very evident in the range of 1020–1010 cm^{-1} and 970–950 cm^{-1} (=C—O—C= stretching). C—H and C=C linkages in aromatic rings showed absorption peaks at 3100–3000 and 1490–1480 cm^{-1}, respectively. The strong absorption bands in the range of 1250–1240 and 1170–1160 cm^{-1}, more intense in the case of polymer **P3**, were linked to the presence of aromatic ether stretchings. Also, polymer **P1** displayed C—F linkage characteristic absorption peaks in the range of 1100–1300 cm^{-1}, while polymer **P2** exhibited phenyl-Si typical absorption bands at 1420, 1105, and 700 cm^{-1}.

Figure 2(b,c) illustrate the ^{1}H NMR and ^{13}C NMR spectra of polyamide **P1**. The assignments of the ^{1}H and ^{13}C chemical shifts were made according to the numbering presented in Figure 2(a) and they were based on 2D NMR experiments.

The NMR data provided evidence for the formation of the amide group. In ^{1}H NMR spectrum of polymer **P1**, the peak corresponding to amide protons is shifted downfield as compared to the peak corresponding to amine protons from the monomer **M1**. The strongest evidence is provided by H,N-HMQC spectra of the polymers, presented in Figure 3. In these spectra, the ^{15}N chemical shift values are in the interval characteristic to secondary amides.

The solubility behavior of these polymers was tested qualitatively in various organic solvents, and the results are summarized in Table 2. All poly(oxadiazole-amide)s were easily soluble at room temperature in polar aprotic solvents (as NMP, DMAc, DMF, and DMSO) and, except for polymer **P3**, even in less polar solvents such as tetrahydrofuran. The improved solubility of these polymers compared with conventional poly(arylene-oxadiazole)s, which are only soluble in strong acids such as H_2SO_4 and methansulfonic acid, and with other poly(oxadiazole-amide)s, which are little soluble in NMP and only in the presence of lithium chloride, can be explained by the presence in the macromolecular chain of flexible ether linkages, voluminous hexafluoroisopropylidene groups or phenyl substituents and the bending of the chains at silicon atoms. These groups prevent the macromolecular chains from packing into tight structures through hydrogen bonds between amide groups and lead to a decreased chain–chain interaction, thus allowing the solvent to penetrate among the polymer chains. Therefore, their excellent solubility makes the present poly(oxadiazole-amide)s potential candidates for practical applications in spin-coating and casting processes.

The molecular weights of the polymers were measured by gel permeation chromatography (GPC), by using polystyrene standards. The molecular weight values, M_n, are in the range of 34,500–53,400 Dalton, M_w in the range of 51,800–95,000 Dalton, and polydispersity M_w/M_n in the domain of 1.47–1.78, a range expected for condensation polymers. The inherent viscosity values of polyamides **P1–P3** were in the range of 0.4–0.5 dL/g (Table 3). As can be seen in Table 3, the present polymers have fairly high values of molecular weight and narrow molecular weight distribution. It should be noted that gel permeation chromatography measurements by using polystyrene standards, which have a completely different structure as compared with the present polyamides,

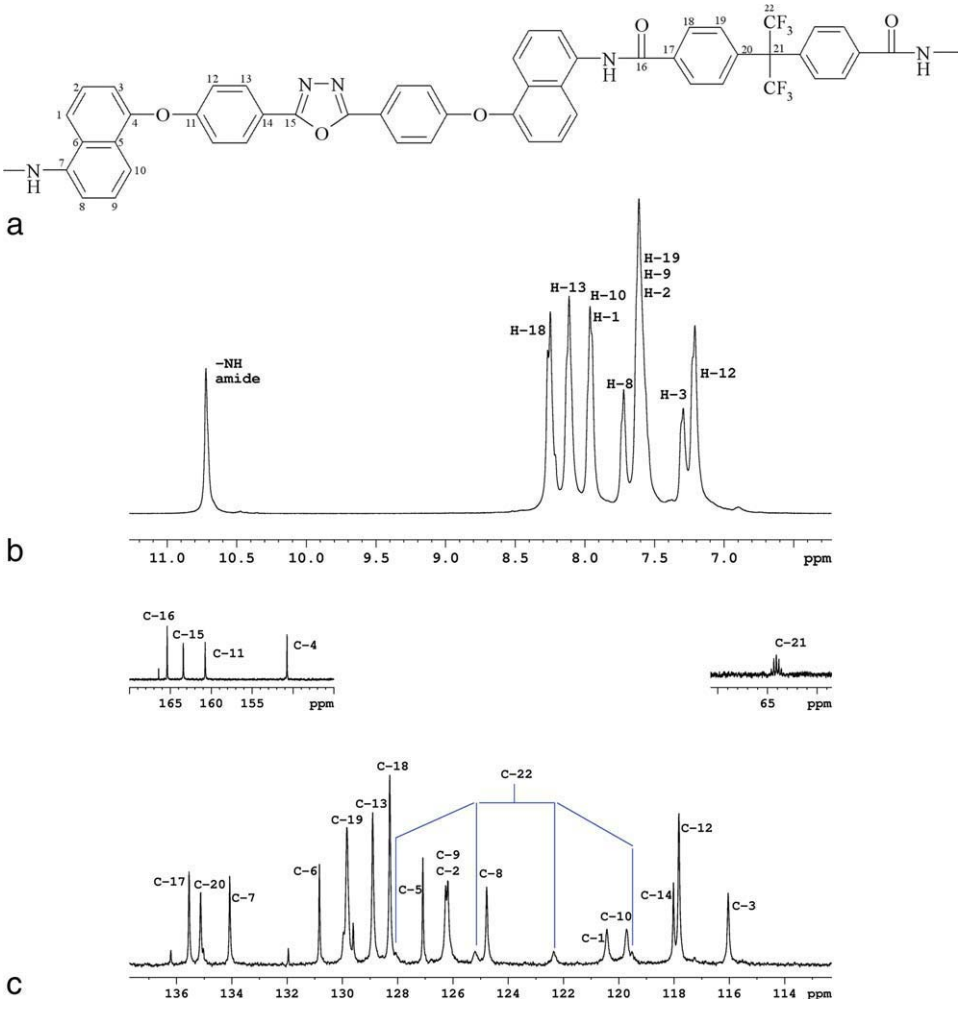

FIGURE 2 NMR spectra of polyamide **P1** in DMSO-d_6: (a) numbering scheme; (b) ^{1}H NMR spectrum; (c) ^{13}C NMR spectrum. [Color figure can be viewed in the online issue, which is available at wileyonlinelibrary.com.]

provide only a crude estimate of molecular weights and not an accurate evaluation.

Thermal Stability

The thermal properties of the poly(oxadiazole-amide)s were evaluated by means of DSC and TGA. The thermal behavior data of the polymers are summarized in Table 4. Representative TGA curves are shown in Figure 4.

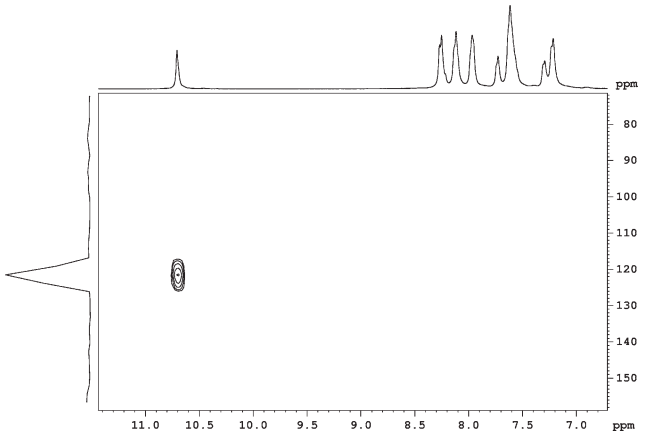

FIGURE 3 H,N-HMQC spectrum of polyamide **P1** in DMSO-d_6.

The polyamides showed T_g values between 248 and 279 °C. As expected, T_g was dependent on the structure of the diacid chloride component and decreased with increasing flexibility of the polymer backbones. The lowest T_g value of polymer **P3** can be explained in terms of flexibility and low rotation barrier of its diacid chloride segment.

The polymers showed excellent thermal stability, as expected in case of aromatic polyamides. The initial decomposition

TABLE 2 Solubility of Polyamides **P1–P3** at Room Temperature

	Solvents				
Polymer	DMF	DMAc	DMSO	NMP	THF
P1	+[a]	+	+	+	+
P2	+	+	+	+	+
P3	+	+	+	+	−[b]

[a] +: Soluble.
[b] −: Insoluble.

TABLE 3 Average Molecular Weights of the Polyamides

Polymer	M_n (Da)	M_w (Da)	PDI	Inherent Viscosity (dL/g)
P1	53,400	95,000	1.78	0.47
P2	49,600	73,300	1.47	0.46
P3	34,500	51,800	1.50	0.40

temperatures (IDT) of the poly(oxadiazole-amide)s were about 395–425 °C and the temperatures of 10% gravimetric loss ($T_{10\%}$), that are important criteria for evaluation of thermal stability, were in the range of 417–467 °C, indicating a high thermal stability. The decomposition of the poly(oxadiazole-amide)s takes place in two steps as shown by DTG curves and by the values of the maximum decomposition temperatures calculated from these curves: the first step occurs in the range 435–495 °C and the second in the range 510–555 °C. The first maximum may be attributed to the degradation of ether linkages nearby the naphthalene units and the second one corresponds to the degradation of oxadiazole rings in the polymer chain. These values are comparable with those of related polyoxadiazoles without any flexible groups,[23] which means that on introducing ether bridges, silicon or hexafluoroisopropylidene units into the main chain of poly(oxadiazole-amide)s the thermal stability was not affected, while the solubility was very much improved. The polymers displayed similar thermal properties with related poly(oxadiazole-amide)s based on the same diacid chlorides and similar diamines, but without naphthalene units.[8] The large interval between decomposition and glass transition of polymers may be useful for the processing of these polymers by thermoforming techniques. This is an important advantage when comparing with related poly(oxadiazole-amide)s, previously reported, which do not have any glass transition.[32]

Film Quality

All these polymers possess film forming ability. The polymer solutions (10%) in NMP were processed into thin films by casting onto glass plates. The free-standing films having a thickness in the range of 20–50 μm were flexible, tough and creasable, and maintained their integrity after repeated bendings. Very thin films having a thickness in the range of 20–50 nm, which have been deposited onto silicon wafers

TABLE 4 Thermal Properties of the Polymers

Polymer	[a] T_g (°C)	[b] IDT (°C)	[c] $T_{10\%}$ (°C)	[d] T_{max1} (°C)	[d] T_{max2} (°C)
P1	279	400	443	476	545
P2	275	425	467	435	510
P3	248	395	417	495	555

[a] T_g: Glass transition temperature.
[b] IDT: Onset on the TG curve.
[c] $T_{10\%}$: Temperature of 10% weight loss on the TG curve.
[d] T_{max}: Temperature of maximum rate of decomposition.

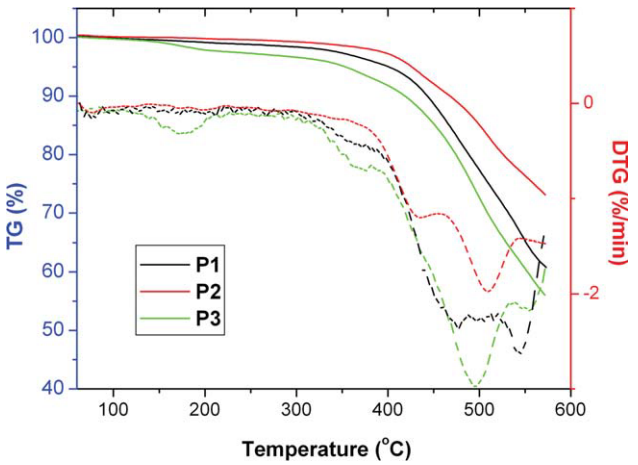

FIGURE 4 TGA (heavy line) and DTG (dashed line) curves of polyamides **P1–P3**. [Color figure can be viewed in the online issue, which is available at wileyonlinelibrary.com.]

exhibited compact, homogeneous surface, without pinholes or cracks, when studied by atomic force microscopy (AFM; Fig. 5). Their root mean square roughness (RMS) is in the range of 4–6 Å being of the same order of magnitude as that of neat, highly polished silicon wafers which have been used as substrates. It means that the present polymer films are very smooth, practically defectless. The films had strong adhesion to silicon wafers: only by scratching with a sharp razor blade small film pieces could be taken off.

Photo-Optical Properties

There is currently much research directed toward the preparation of blue light-emitting polymers, because blue light can be converted to green or red using the proper dyes, which means a blue light-emitting device alone is capable of generating all colors, while green or red cannot emit blue light by this method. Moreover, blue light is difficult to be attained with the already known inorganic electroluminescent materials. In this regard, the 1,3,4-oxadiazole rings are promising chemical moieties for introduction into the polymer backbone or in the pendant structure.[33] In addition, the use of electroluminescent thin films made from highly thermostable polymers would avoid the thermal degradation in the final device while in service at elevated temperatures. Since 1,3,4-oxadiazole rings and naphthalene units are known as light-emissive,[34] the light-emitting properties of polyamides **P1-P3** containing these chromophores have been investigated. The light-emitting ability was assessed on the basis of the photoluminescence (PL) spectra which were recorded for both polymer solutions in NMP and polymer films cast from NMP solutions, after excitation with UV light of different wavelengths. The UV–vis and PL spectra of poly(oxadiazole-amide)s **P1–P3** are displayed in Figures 6 and 7.

The prominent feature in these materials is their extended conjugated π-system; such extension is mirrored by the electronic absorption spectrum. All the polyamides displayed one strong UV absorption maximum in NMP solution, at about 312 nm, their spectra being quite identical (Fig. 6).

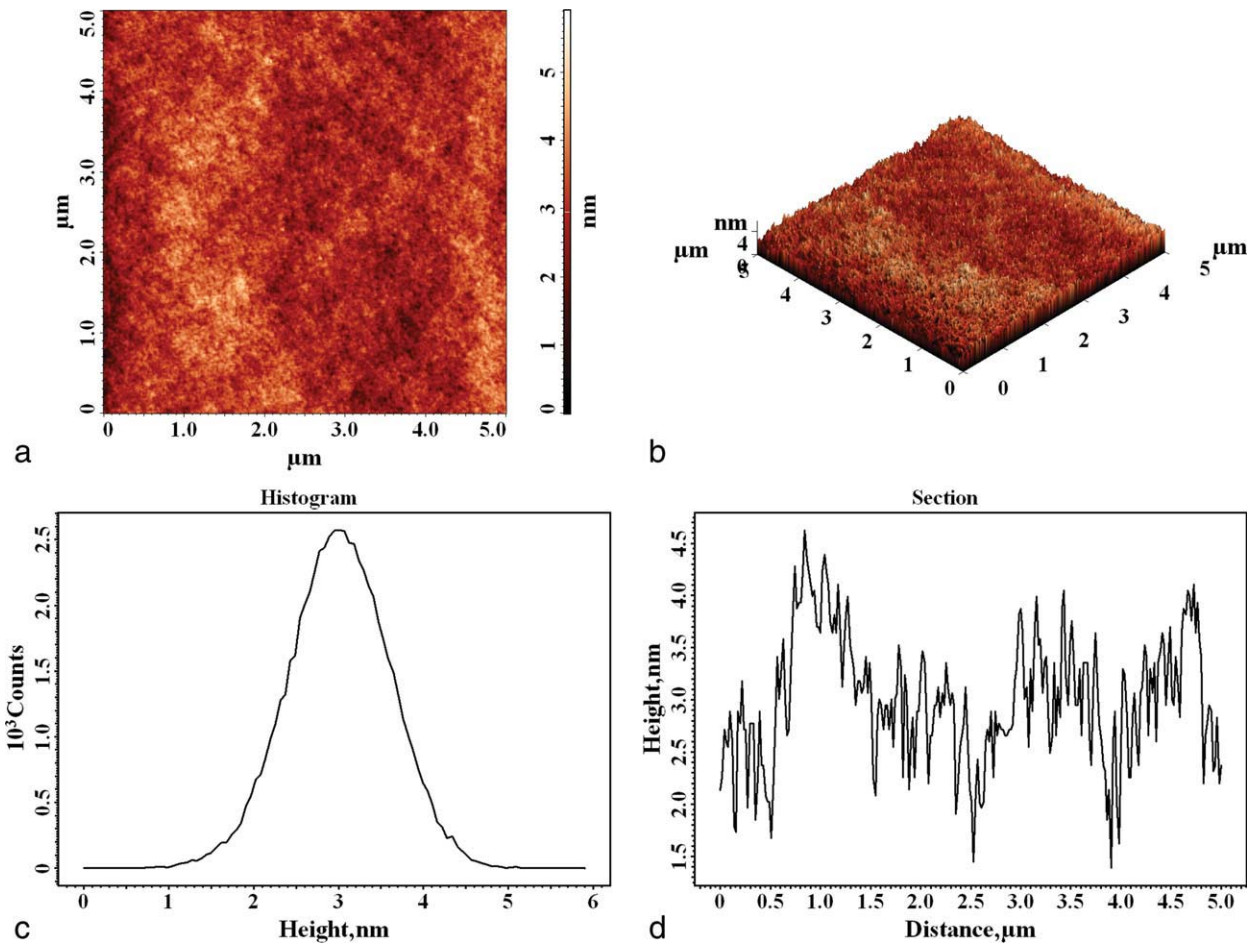

FIGURE 5 AFM images of polyamide **P3** film on silicon wafer (a, top view; b, side view; c, histogram; d, section).

The absorption maximum of these polymers is mainly determined by the diphenyl-1,3,4-oxadiazole unit, because the unsubstituted diphenyl-1,3,4-oxadiazole in hexane shows its absorption maximum at 284 nm.[35] Due to the substitution of the phenylene rings in *para*-position with oxygen, the absorption is slightly red shifted to about 310 nm. In the ground state the oxygen behaves just like a weak conjugation bridge because the difference in absorption, which depends on the substitution position of the nearby naphthalene at the oxygen, is very weak. In the excited state, the oxygen acts as

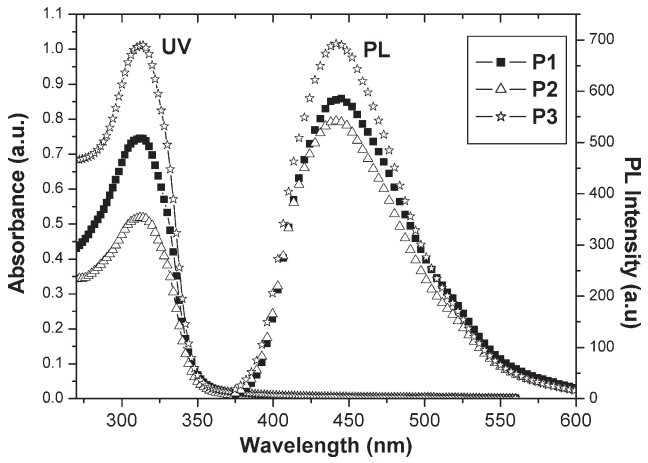

FIGURE 6 UV–vis and PL spectra of polyamides in NMP solutions.

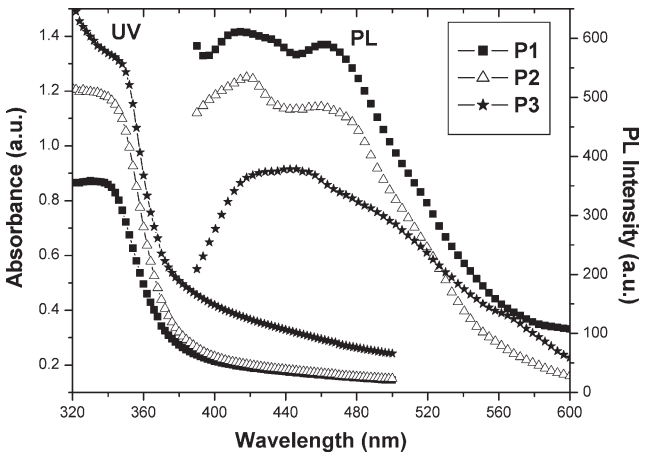

FIGURE 7 UV–vis and PL spectra of polyamides in solid state.

TABLE 5 Optical Properties of Poly(oxadiazole-amide)s in Solution and Solid State

Polymer	UV, sol λ_{abs} (nm)	UV, sol λ_{edge} (nm)	UV, film λ_{abs} (nm)	UV, film λ_{edge} (nm)	$E_{g,sol}$ (eV)	$E_{g,film}$ (eV)
P1	312	363	343	378	3.42	3.28
P2	312	361	346	380	3.43	3.26
P3	314	362	350	371	3.43	3.34

λ_{abs}: Wavelength of the maximum absorption peak.
λ_{edge}: Wavelength of the absorption edges (onset) of the optical absorption spectra.
E_g: Energy band gap.
s: Shoulder.

a better bridge for the delocalization of the charge, because the position of the naphthalene ring next to the oxygen determines the photoluminescence more significantly.

In films cast from NMP solution all polyamides presented one absorption maxima (shoulder) in the range of 343–350 nm (Fig. 7) that can be attributed to π-π^* transitions involving oxadiazole-naphthalene framework. The absorbance spectra of solutions and thin films allow us to compare the position of absorption bands λ_{abs}, as seen in Table 5. The red-shift (31–38 nm) of the absorption maxima in solid state with respect to solution could be explained by the fact that the surrounding chromophore polarity became weaker, and the intermolecular interaction of the polymer backbones became stronger. The absorption edge, being a long-wavelength wing of the longest-wavelength band of the spectrum, moves to longer wavelength (smaller energy) for the polymer film when compared with the solution of the same polymer. This means that conformation of polymer chain can be different depending on the surroundings.[36]

The energy band gap (E_g) could be estimated from the following equation:

$$E_g = h \times c/\lambda_{edge}$$

where h is the Planck constant, c is the light velocity, and λ_{edge} is the wavelength of the absorption edges of the optical absorption spectra. This simple method allows estimating and then comparing the energy gaps for the investigated polymers in the form of solution and thin film, as it is gathered in Table 5. The energy gap of poly(oxadiazole-amide)s **P1–P3** varies from 3.42 to 3.43 eV for polymer solutions and from 3.26 to 3.34 eV for polymer films. The E_g values in solution do not seem to be influenced by the nature of the diacid chloride segment of the polymer chain. The E_g values of the polyamide films are smaller than the E_g values of the corresponding polymer solutions, due to the more aggregated conformation of polymer main chains in solid state. For the polymer films, the highest energy bandgap was found for **P3** containing ether bridges in the diacid chloride segment and the smallest energy bandgap was found for **P2** incorporating silicon atom in the macromolecule, which do not disturb the conjugation along the main chain.

The most striking feature was that all these polymers in solution emitted an intense blue color upon irradiation with UV light, with the highest intensity of luminescence in solution corresponding to polymer **P3**. The emission maximum was centered on 440 nm (Fig. 6) and it was determined by the nature of the new monomer, particularly by the oxadiazole and naphthalene chromophores. All the polymers showed one shoulder at ~520 nm due to negligible intermolecular interactions of the conjugated parts of the polymer chains. Maximum emission wavelength along with Stokes shift values of these polymers are collected in Table 6. The introduction of ether bridges, silicon or hexafluoroisopropylidene units into the main chain of poly(oxadiazole-amide)s did not affect the wavelength of the PL emission in solution, while it had an important influence on the solubility and processability of the polymers.

The PL spectra of the films cast from NMP solutions of these poly(oxadiazole-amide)s containing oxadiazole and naphthalene chromophores showed the main maxima in the blue spectral range, at 413–420 nm and 445–465 nm, and small peaks or shoulders at 433 nm and 498 nm in the case of polymers **P1** and **P3**, respectively (Fig. 7; Table 6). The maximum from 413–420 nm can be attributed to phenyl-oxadiazole emitter while the maximum from 445–465 can be due to the naphthalene-containing chain segments. The small peak at 433 nm and the shoulder at 498 nm in the PL spectra of the polyamide films **P1** and **P3**, respectively, are due to the various degrees of aggregation and the excimer formation in the films, leading to photoluminescence quenching, emission band broadening, and bathochromic shift.[37] Interestingly, while most conjugated polymers exhibit bathochromic shifts from solution to solid state, the emission spectra of polymers **P1–P3** exhibit hypsochromic shifts in thin films,

TABLE 6 PL Properties of Poly(oxadiazole-amide)s **P1–P3**

	Solution		Films	
Polymer	PL λ_{em} (nm)	Stokes Shift	PL λ_{em} (nm)	Stokes Shift
P1	444, 522^s	132	413, 433, 464	70
P2	440, 521^s	128	420, 465	74
P3	441, 523^s	127	420, 445, 498^s	70

λ_{em}: Wavelength of the maximum PL emission peak.
s: Shoulder.

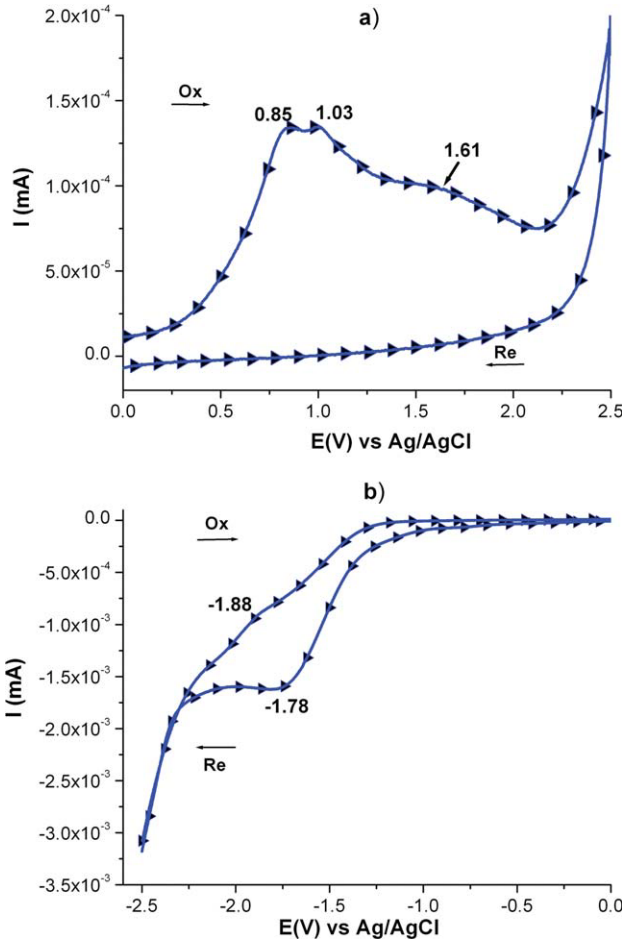

FIGURE 8 The first CV scan of the cast film of polyamide **P1** on ITO coated glass substrate (a, anodic scan; b, cathodic scan). [Color figure can be viewed in the online issue, which is available at wileyonlinelibrary.com.]

which is indicative of a solid-state organization that disrupts the extent of conjugation.[38] The Stokes shift (the difference between the main fluorescence and UV–vis peaks) are in the range of 127–132 nm for polymer solutions and 70–74 for polymer films. It is known that if the Stokes shift is too small, the emission and absorption spectra will overlap more, and the emitted light will be self-absorbed and the luminescence efficiency will decrease in the device. All these poly(oxadiazole-amide)s display enough high values of the Stokes shift for good luminescence efficiency. Therefore these polymer films are promising candidates for application as emitting materials in blue light-emitting devices.

Electrochemical Characterization

The electrochemical properties of poly(oxadiazole-amide)s **P1–P3** were investigated by CV for cast films on ITO-coated glass substrates as a working electrode in dry acetonitrile (MeCN) containing 0.1 M of tetrabuthylamonium perchlorate (TBAP) as electrolyte salt, under nitrogen atmosphere. The cyclic voltammograms of polyamide **P1** recorded at a scan rate of 100 mV/s are shown in Figure 8 (a: anodic scan; b: cathodic scan).

The CV diagrams indicate three irreversible oxidation processes at anodic peak potentials (E_{pa}) of 0.85 V (E_{onset}^{ox} = 0.53 V), 1.03 V and 1.61 V, respectively, and one reversible reduction redox couple at cathodic peak potentials E_{pc}^{red} of −1.78 V (E_{onset}^{red} = −1.33 V) and E_{pc}^{ox} of −1.88 V. The electron removal in the first two stages of oxidation process for polyamide **P1** is assumed to occur at the N atom surrounded by naphthalene and phenyl groups due to the electron-donating amide linkages in the main chain, leading to the formation of radical cations. The third peak, at 1.61 V, can be ascribed to oxidation of phenoxy groups, causing radical recombination and formation of a dication having a quinoid structure. The third oxidation step is stable since no change in the position of the anodic peak and only the current intensity increase was observed (Fig. 9). However, the other oxidation steps and reduction processes seemed to be not very stable as that of the first one. As shown in Figure 9, the redox waves of polymer **P3** showed a slight shift of the

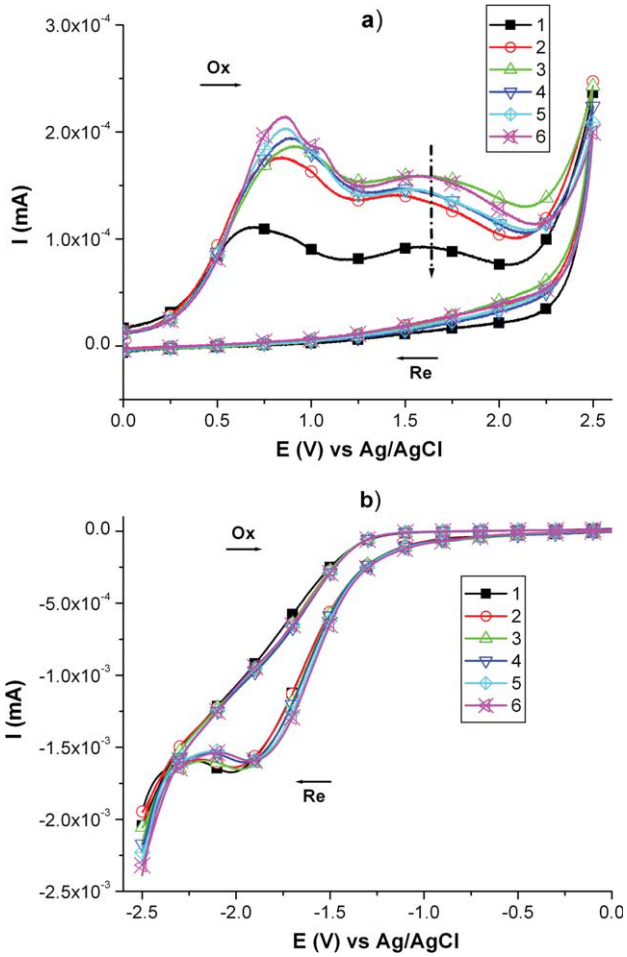

FIGURE 9 Repetitive CV scan of the polyamide **P3** film on an ITO electrode in 0.1 M TBAP/MeCN solution (6 cycles; a, anodic scan; b, cathodic scan). [Color figure can be viewed in the online issue, which is available at wileyonlinelibrary.com.]

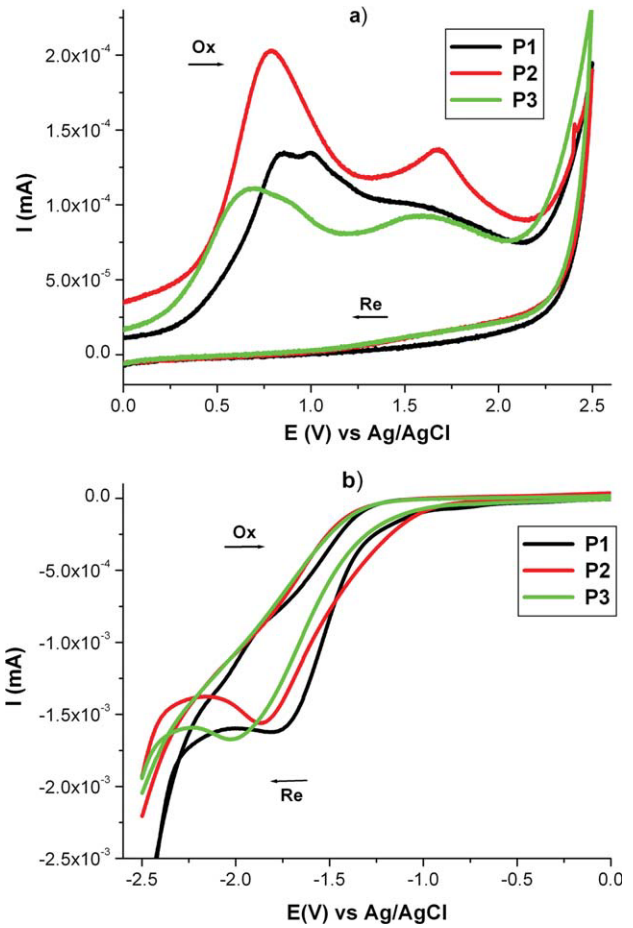

FIGURE 10 Cyclic voltammograms of the cast films of polyamides **P1–P3** on ITO-coated glass substrate in 0.1 M TBAP/MeCN solution at a scan rate of 100 mV/s (a, anodic scan; b, cathodic scan). [Color figure can be viewed in the online issue, which is available at wileyonlinelibrary.com.]

anodic/cathodic peaks and a slight increase/decrease in current density after six cyclic scans in a potential range of −2.5 up to +2.5 V at the scan rate of 100 mV/s. The oxidation of those polyamide films is accompanied by no colour changes.

Figure 10 compares the CV curves of structurally similar polyamides **P1, P2,** and **P3**. While polyamides **P1** and **P3** showed similar oxidation redox waves, due to the high electronegative surroundings of the amide groups (ether or hexafluoroisopropylidene), the polyamide **P2** displayed only two well defined oxidation peaks at 0.79 and 1.68 eV due to the lower electronegativity of diphenylsilane unit that limits the formation of electrochemical species. Also, it can be observed a large current intensity increase in the oxidation CV waves of polyamide **P2** as compared with **P1** and **P3**. In contrast with poly(oxadiazole-amide)s **P1** and **P3** that exhibit an interruption of electron conjugation along the macromolecule, the silicon atom incorporated into the main chain of polyamide **P2** does not disturb the conjugation and supports the transport of electronic charges.[39] The cathodic peaks at −1.78 V (vs. Ag/AgCl) and −1.88 V (vs. Ag/AgCl) for polyamide **P1** can be attributed to the reduction and oxidation, respectively, of oxadiazole rings. Polyamides **P2** and **P3** did not show the redox peaks corresponding to the oxidation of oxadiazole ring.

The energy levels of the highest occupied molecular orbital (HOMO) and lowest unoccupied molecular orbital (LUMO) of the investigated polyamides can be determined from the oxidation onset potentials (E_{onset}^{ox}) and reduction onset potentials (E_{onset}^{red}) versus Ag/AgCl. The onset potentials were determined from the intersection of the two tangents drawn at the rising current and baseline charging current of the CV curves. The external ferrocene/ferrocenium (Fc/Fc^{+}) redox standard E_{onset} is 0.425 V versus Ag/AgCl in MeCN. Assuming that the HOMO energy for the Fc/Fc^{+} standard was 4.80 eV with respect to the zero vacuum level, we can estimate the HOMO energy levels of polyamides **P1-P3** (in electron volts, eV) according to the equation reported by Li et al.[40] Thus, $E_{LUMO} = E_{onset}^{red} + 4.37$ and $E_{HOMO} = E_{onset}^{ox} + 4.37$ and the value of energy gap, $E_g = E_{HOMO} - E_{LUMO}$. The energy level values and the energy gap characteristics of polyamides containing oxadiazole rings in the main chain, **P1–P3**, are summarized in Table 7.

The HOMO and LUMO energy levels of the materials are very crucial parameters for electroluminescence device configuration. The LUMO energy values of these poly(oxadiazole-amide)s was thus determined to be in the range of 3.04–3.27 eV. These values are almost the same as that of cyano-polyphenylenevinylene (CN-PPV) (3.02 eV) and other aromatic polyoxadiazoles (2.8–3.2 eV), which all exhibit good electron-injection properties.[34] The HOMO energy level was

TABLE 7 Electrochemical Properties of Poly(oxadiazole-amide)s

Polymer	E_{onset}^{ox} (V)	E_{pa}^{1} (V)	E_{pa}^{2} (V)	E_{pa}^{3} (V)	E_{onset}^{red} (V)	E_{pc}^{red} (V)	E_{pc}^{ox} (V)	E_{HOMO} (eV)	E_{LUMO} (eV)	E_g (eV)
P1	0.53	0.85	1.03	1.61	−1.33	−1.78	−1.88	4.9	3.04	1.86
P2	0.42	0.79	1.68	–	−1.10	−1.86	–	4.79	3.27	1.52
P3	0.30	0.68	0.90	1.60	−1.32	−2.02	–	4.67	3.05	1.62

E_{onset}^{ox}: Oxidation onset potential.
E_{onset}^{red}: Reduction onset potential.
E_{pa}: Anodic peak potential.
E_{pc}: Cathodic peak potentiall.
E_{HOMO}: The HOMO energy levels.
E_{LUMO}: The LUMO energy levels.
E_g: Energy gap measured from electrochemical data according to the E_{onset}.

estimated to be in the range of 4.67-4.9 eV. These values are comparable with that of methoxy-ethyl-hexyloxy-polyphenylenevinylene (MEH-PPV) (4.87 eV),[41] that display a very good hole injection ability. The energy barriers between the emitting polymers and electrodes can be estimated by comparing the work functions of electrodes with the highest occupied molecular orbital (HOMO) or the lowest unoccupied molecular orbital (LUMO) of emitting polymers. Thus, the hole injection barrier is $\Delta E_h = E_{HOMO} - 4.8$ (eV) (4.8 eV is the work function of the ITO anode), whereas the electron injection barrier is $\Delta E_e = 4.3 - E_{LUMO}$ (eV), where 4.3 eV is the work function of aluminum cathode. The difference between the electron and hole injection barriers ($\Delta E_e - \Delta E_h$) is a useful parameter for evaluating the balance in the two injections. Lower ($\Delta E_e - \Delta E_h$) values mean improved injection balance of electrons and holes from the cathode and anode, respectively. The band structures of **P1–P3** and poly(*p*-phenylenevynilene) (**PPV)** are depicted together in Figure 11 for comparison, and the barrier energies are listed in Table 8.

It is evident that the presence of 1,3,4-oxadiazole rings in all these polymers decrease the energy barrier for electron injection from Al electrode to the polymer layer. In the same time, the amide groups surrounded by phenyl and naphthalene units decrease the energy barrier for hole injections in the present poly(oxadiazole-amide)s. The ΔE_e, ΔE_h, and ($\Delta E_e - \Delta E_h$) of **P2** are lower than those of **P1** and **P3** due to the presence of silicon atom in the polymer chains that do not disturb the conjugation. However, the barrier energy differences ($\Delta E_e - \Delta E_h$) of the poly(oxadiazole-amide)s **P1, P2,** and **P3** are lower than those of **PPV** by values of 0.24, 0.36, and 0.28 eV, respectively. As a general conclusion, our polymers are excellent candidates for electroluminescence devices (LEDs), presenting very good electron and hole injection properties and very low barrier energy between electron injection and hole injection from electrodes to polymer, the poly(oxadiazole-amide) **P2** being the best one.

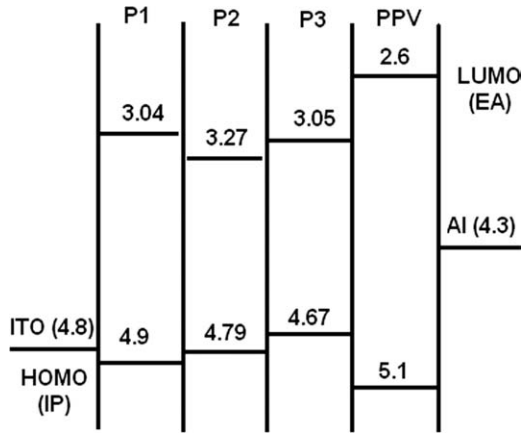

FIGURE 11 Band diagrams of **P1–P3** and **PPV** as determined from electrochemical data.

TABLE 8 The Barrier Energies of **P1–P3** and **PPV**

Polymer	ΔE_h	ΔE_e	$\Delta E_e - \Delta E_h$
P1	0.1	1.26	1.16
P2	0.01	1.03	1.02
P3	0.13	1.25	1.12
PPV[a]	0.30	1.70	1.40

ΔE_h: Barrier energy for hole injection from ITO to polymer.
ΔE_e: Barrier energy for electron injection from Al to polymer .
$\Delta E_e - \Delta E_h$: The difference of barrier energy between electron injection and hole injection from electrodes to polymer.
[a] From ref. 42.

CONCLUSIONS

Design and synthesis of a new aromatic diamine containing 1,3,4-oxadiazole and naphthalene rings and of new thermally stable polyamides based on it with improved solubility and interesting optical properties was the main objective of this work. A novel diamine, namely 2,5-bis-[4-(5-amino-naphthalene-1-yloxy)-phenyl]-1,3,4-oxadiazole, was successfully prepared by aromatic nucleophilic substitution reaction of 2,5-bis(*p*-fluorophenyl)-1,3,4-oxadiazole with 5-amino-1-naphthol, in the presence of K_2CO_3. This compound was characterized by elemental analysis, MS, IR, ^{1}H NMR, and ^{13}C NMR spectroscopy, fully confirming the chemical structure of the monomer. Low-temperature solution polycondensation reactions of this diamine with aromatic diacid chlorides resulted in preparation of different poly(oxadiazole-amide)s with a nice balance of properties, thermal stability versus solubility. All polyamides were easily soluble at room temperature in polar aprotic solvents and, except for one of them, they were soluble even in less polar solvents such as tetrahydrofuran. The polymers showed excellent thermal stability, up to 395 °C, and displayed glass transition in the range of 248–279 °C, with a large interval between decomposition and glass transition temperatures that make these polyamides appropriate for processing by a thermoforming technique, as well. All the polymers, both in solution and in solid state, emitted an intense blue color upon irradiation with UV light. These polymers exhibit very good electron and hole injection properties and very low barrier energy between electron injection and hole injection from electrodes to polymer, thus being promising for application in electroluminescent devices. Further research is necessary to study their use and performance in blue-light-emitting devices. Therefore, the new diamine containing oxadiazole and naphthalene rings provides an important guideline for the design of new alternating copolymers that can be used to fabricate light-emitting materials.

One of the authors (M. D. Damaceanu) acknowledges the financial support of European Social Fund "Cristofor I. Simionescu" Postdoctoral Fellowship Programme (ID POSDRU/89/1.5/S/55216), Sectoral Operational Programme Human Resources Development 2007-2013. The authors are grateful to Dr. Loredana Vacareanu from "Petru Poni"' Institute of

Macromolecular Chemistry, Iasi-Romania, for the cyclic voltammetry measurements of the polymers.

REFERENCES AND NOTES

1 García, J. M.; García, F. C.; Serna, F.; de la Peña, J. L. Prog Polym Sci 2010, 35, 623–686.

2 Preston, J. In Encyclopedia of Polymer Science and Engineering; Mark, H. F., Bikales, N. M., Overberger, C. C., Menges, G., Eds.; Wiley: New York, 1988; Vol. 11, pp 381–409.

3 Vollbracht, L. In Comprehensive Polymer Science; Allen, G., Bevington, J. C., Eastmond, G. C., Ledwith, A., Russo, S., Sigwald, P., Eds.; Pergamon Press: Oxford, 1989; Vol. 5, pp 375–386.

4 Saifrasun, S.; Amornsakchai, T.; Sirisinha, C.; Meesiri, W.; Bualek-Limcharoen, S. Polymer 1999, 40, 6437–6442.

5 Kricheldorf, H. R.; Schmidt, B. Macromolecules 1992, 25, 5471–5476.

6 Kricheldorf, H. R.; Burger, R. J Polym Sci Part A: Polym Chem 1994, 32, 355–362.

7 Hsiao, S. H.; Liou, G. S.; Kung, Y. C.; Hsiung, T. J Polym Sci Part A: Polym Chem 2010, 48, 3392–3401.

8 Iosip, M. D.; Bruma, M.; Robison, J.; Kaminorz, Y.; Schulz, B. High Perform Polym 2001, 13, 133–148.

9 Calderón, V.; García, F. C.; de la Peña, J. L.; Maya, E. M.; García, J. M. J Polym Sci Part A: Polym Chem 2006, 44, 2270–2281.

10 Calderón, V.; García, F.; de la Peña, J. L.; Maya, E. M.; Lozano, A. E.; de la Campa, J. G.; de Abajo, J.; García, J. M. J Polym Sci Part A: Polym Chem 2006, 44, 4063–4075.

11 García, J. M.; García, F.; Sanz, R.; de la Campa, J. G.; Lozano, A. E.; de Abajo, J. J Polym Sci Part A: Polym Chem 2001, 39, 1825–1832.

12 Gaudiana, R. A.; Minns, R. A.; Rogers, H. G.; Sinta, R.; Kalganarama, P.; McGrown, C. J Polym Sci Part A: Polym Chem 1987, 25, 1249–1271.

13 Ayala, V.; Maya, E. M.; García, J. M.; de la Campa, J. G.; Lozano, A. E.; de Abajo, J. J Polym Sci Part A: Polym Chem 2005, 43, 112–121.

14 Staubli, A.; Mathiowitz, E.; Langer, R. Macromolecules 1991, 24, 2291–2298.

15 Ueda, M.; Morishima, M.; Kakuta, M.; Sugiyama, J. Macromolecules 1992, 25, 6580–6585.

16 Nakata, S.; Brisson, J. J Polym Sci Part A: Polym Chem 1997, 35, 2379–2386.

17 García, J. M.; García, F. C.; Serna, F. J Polym Sci Part A: Polym Chem 2003, 41, 1202–1215.

18 Yang, C. P.; Lin, J. H. J Polym Sci Part A: Polym Chem 1994, 32, 369–382.

19 Yang, C. P.; Hsiao, S. H.; Chen, K. H. Polymer 2002, 43, 5095–5104.

20 Liou, G. S.; Hsiao, S. H.; Ishida, M.; Kakimoto, M.; Imai, Y. J Polym Sci Part A: Polym Chem 2002, 40, 3815–3822.

21 Yang, C. P.; Su, Y. Y. J Polym Sci Part A: Polym Chem 2004, 42, 222–236.

22 Wang, K. L.; Liu, Y. L.; Lee, J. W.; Neoh, K. G.; Kang, E. T. Macromolecules 2010, 43, 7159–7164.

23 Schulz, B.; Bruma, M.; Brehmer, L. Adv Mater 1997, 9, 601–613.

24 Bruma, M.; Kőpnick, T. Adv Colloid Interface Sci 2005, 116, 277–290.

25 Damaceanu, M. D.; Musteata, V. E.; Cristea, M.; Bruma, M. Eur Polym J 2010, 46, 1049–1062.

26 Damaceanu, M. D.; Rusu, R. D.; Bruma, M.; Jarzabek, B. Polym J 2010, 42, 663–669.

27 Iosip, M. D.; Bruma, M.; Ronova, I.; Szesztay, M.; Muller, P. Eur Polym J 2003, 39, 2011–2021.

28 Zhu, S.; Schulz, B.; Bruma, M.; Brehmer, L. Polym Adv Technol 1996, 7, 879–887.

29 Hamciuc, E.; Hamciuc, C.; Bruma, M.; Schulz, B. Eur Polym J 2005, 41, 2989–2997.

30 Bruma, M.; Schulz, B.; Mercer, F. J Macromol Sci Pure Appl Chem A 1995, 32, 259–286.

31 Thaemlitz, C. J.; Cassidy, P. E. Polymer 1992, 33, 206–208.

32 Bruma, M.; Schulz, B.; Kopnick, T.; Robison, J. High Perform Polym 2000, 12, 429–443.

33 Segura, J. L. Acta Polym 1998, 49, 319–344.

34 Akcelrud, L. Prog Polym Sci 2003, 28, 875–962.

35 Hill, J. In Comprehensive Heterocyclic Chemistry; Katritzky, A. R., Rees, C. W., Eds.; Pergamon Press: Oxford, 1989; Vol. 6, Chapter 4, pp 427–446.

36 Sek, D.; Iwan, A.; Jarzabek, B.; Kaczmarczyk, B.; Kasperczyk, J.; Mazurak, Z.; Domanski, M.; Karon, K.; Lapkowski, M. Macromolecules 2008, 41, 6653–6663.

37 Zhan, X.; Liu, Y.; Wu, X.; Wang, S.; Zhu, D. Macromolecules 2002, 35, 2529–2537.

38 Bouffard, J.; Swager, T. M. Macromolecules 2008, 41, 5559–5562.

39 Schulz, B.; Janietz, S.; Sava, I.; Bruma, M. Polym Adv Technol 1996, 7, 514–518.

40 Li, Y.; Cao, Y.; Gao, J.; Wang, D.; Yu, G. J. Synth Met 1999, 99, 243–248.

41 Cervini, R.; Li, X.; Spencer, G. W. C.; Holmes, A. B.; Moratti, S. C.; Friend, R. H. Synth Met 1997, 84, 359–360.

42 Bradley, D. D. C. Synth Met 1993, 54, 401–415.